18th Brazilian Congress of Thermal Sciences and Engineering
November 16–20, 2020 (Online)

# ENC-2020-0289
# ANALYSIS OF THERMAL RADIATION MODELS IN THE PRESENCE OF DIFFERENT LEVELS OF TURBULENT FLUCTUATIONS

**Bruno de Luca Zimmer Gomes**
**Guilherme Crivelli Fraga**
**Francis Henrique Ramos França**
Universidade Federal do Rio Grande do Sul, Department of Mechanical Engineering - Rua Sarmento Leite, 425, Porto Alegre, Brazil
bruno.luca@ufrgs.br; guilhermecfraga@gmail.com; frfranca@ufrgs.br

***Abstract.*** *In turbulent reactive fluxes, it is important to include the effects of the Turbulence-Radiation interaction (TRI). If not included, it can lead to large errors in the predicted radiant heat flow and in the radiation fraction of the flame. The objective of this paper is to test the accuracy of the different WSGG models under the effects of TRI when compared to the Line-by-line integration (LBL) method. The WSGG models were tested for three different levels of turbulence intensity (TI):* 0 %, 40 % *and* 60 %*. The WSGG models that were analyzed showed an average of* 5 % *in the differences between the models and the LBL benchmark solution for both the source term and the radiative heat flux. There is slight improvement in the accuracy of the WSGG models with the increase in the turbulence intensity. This study brings as a contribution the investigation of the turbulence effects in reactive flows. The results are discussed based on the accuracy of the analyzed WSGG models.*

***Keywords:*** *turbulence-radiation-interaction, thermal radiation, temperature fluctuations, spectral models.*

## 1. INTRODUCTION

Turbulence-Radiation-Interaction (TRI) combines the challenges of thermal radiation and turbulence modeling, the former being the main heat transfer mechanism for high-temperatures applications, the latter being the most common regime of fluid flow. For turbulent reacting flows, TRI effects are known to be important, to be important neglecting this effects can lead to errors of more than one order of magnitude in the prediction of radiative heat fluxes and radiant fraction of flames (Coelho, 2007).

Even in laminar flows, or when the radiative transfer is solved in a decoupled manner from the other physical processes, a major challenge in modeling the radiation exchange is capturing how the radiative properties of a participating medium (i.e., a medium that emits, absorption and/or scatter radiative energy) vary with the radiation spectrum. Several spectral models have been developed for this purpose, encompassing different levels of complexity, computational cost and accuracy. However, considering that turbulence affects distinct regions of the radiation spectrum in different manners (Hall and Vranos, 1994), it may be the case that the performance of these spectral models are not be the same when evaluated in the presence or absence of turbulent fluctuations. In spite of this, to the best knowledge of the present authors, there has not been much effort in including TRI effects in evaluations of the accuracy of spectral models.

A notable exception is the series of studies by Krishnamoorthy and collaborators (Krishnamoorthy, 2012, 2010; Krishnamoorthy *et al.*, 2005b,a),, which attempted to incorporate the effect of turbulent fluctuations in the evaluation of non-gray and gray gas radiation models. In those studies, only TRI effects on the radiative emission were considered, and were modeled through a simple approximation developed by Snegirev, 2004, that determines the mean emission in terms of the mean temperature, mean species concentrations and temperature variance. Absorption TRI was neglected by invoking the optically thin fluctuation approximation, OTFA (Kabashnikov and Kmit, 1979).

In this framework, the present study analyzes the accuracy of different weighted-sum-of-gray-gases (WSGG) models, in the presence of turbulent fluctuations. The reference for the calculations is provided by the line-by-line (LBL) integration methodology, which is applied based on the high-resolution spectral HITEMP2010 database (Rothman *et al.*, 2010). The analyses are carried out for a one-dimensional medium slab with prescribed temperature, medium composition and temperature variance fields (the latter being important for incorporating the effects of turbulence on the results). The temperature and medium composition profiles are the same as in a previous paper (Dorigon *et al.*, 2013), which also studied the accuracy of the WSGG model, but without considering the effect of turbulent fluctuations.

## 2. THEORETICAL BASIS

### 2.1 Thermal radiation in participating media

The radiative transfer equation (RTE) describes the variation of the spectral radiation intensity, $I_\eta$, along an optical path $s$. For a non-scattering medium, as it is considered in all cases studied here (following Dorigon *et al.*, 2013) the RTE is given by (Modest, 2013)

$$\frac{\mathrm{d}I_\eta}{\mathrm{d}s} = -\kappa_\eta I_\eta + \kappa_\eta I_{b\eta} , \quad (1)$$

where $I_{b\eta}$ is the spectral blackbody radiation intensity or Planck function, $\kappa_\eta$ is the spectral absorption coefficient, and $\eta$ denotes the dependence on the radiation spectrum. In this equation, note that the first and second terms on the right-hand side represent the radiative energy locally absorbed by and emitted by the medium, respectively.

It is important to highlight for later use the spectrally-integrated form of Eq. (1), which is given as

$$\frac{\mathrm{d}I}{\mathrm{d}s} = -\kappa_G I + \kappa_P I_b . \quad (2)$$

In this equation, $I$ and $I_b$ are the total local intensity and blackbody intensity (i.e., $I = \int_0^\infty I_b \,\mathrm{d}\eta$ and $I_b = \int_0^\infty I_{b\eta} \,\mathrm{d}\eta$), and $\kappa_G$ and $\kappa_P$ are the incident-mean and Planck-mean absorption coefficients, respectively, which to ensure the consistency of the formulation, are defined as $\kappa_G = \int_0^\infty \kappa_\eta I_\eta \,\mathrm{d}\eta \,/I$ and $\kappa_P = \int_0^\infty \kappa_\eta I_{b\eta} \,\mathrm{d}\eta \,/I_b$.

### 2.2 Line-by-line (LBL) integration

Note that if full knowledge is available pertaining to the dependence of the spectral absorption coefficient $\kappa_\eta$ on the local thermodynamic state and on the radiation wavenumber, Eq. (1) can be solved directly (subjected to an appropriate boundary condition), so that the total intensity can be determined by integrating the resulting spectral intensity. This is the so-called line-by-line (LBL) integration method, which is regarded as the most accurate solution approach for the spectral part of the radiative transfer problem, and is often used as the benchmark for evaluations of spectral models (see, e.g., Kangwanpongpan *et al.* (2012); Dorigon *et al.* (2013); Bordbar *et al.* (2014); Cassol *et al.* (2014)).

In this paper, all information on $\kappa_\eta$ is taken from the HITEMP 2010 database (Rothman *et al.*, 2010). The absorption spectra of $H_2O$ and $CO_2$ (the only species considered to participate in the radiative transfer process for the present calculations) are extracted for 150 000 spectral intervals between $\eta = 0\,\mathrm{cm}^{-1}$ and $\eta = 10^4\,\mathrm{cm}^{-1}$, yielding a spectral resolution of $0.067\,\mathrm{cm}^{-1}$. Spectral line broadening is described by the Lorentz profile, adopting a line-wing cutoff of $40\,\mathrm{cm}^{-1}$ for water vapor and $800\,\mathrm{cm}^{-1}$ for carbon dioxide. For $H_2O$, the absorption spectra are constructed at partial pressures of 0.01 atm, 0.1 atm, 0.2 atm and 0.4 atm (the total pressure is always set to 1.0 atm), with linear interpolation adopted for intermediary partial pressures; for $CO_2$, since it does not present a significant self-broadening effect (Howell *et al.*, 2016), the spectrum for any partial pressure is determined by linear interpolation of data produced at 0.1 atm. For the temperature, the spectral data are generated for temperatures between 400 K and 2400 K, in intervals of 100 K, and linear interpolation is again adopted for intermediary temperatures. More information on the procedure to obtain the $H_2O$ and $CO_2$ absorption lines is given in Dorigon *et al.*, 2013; Cassol *et al.*, 2014.

### 2.3 The weighted-sum-gray-gases (WSGG) model

The WSGG model replaces the complex absorption spectrum of a participating medium by a small set of $J$ gray gases with constant absorption coefficient that occupy non-contiguous spectral intervals, and transparent windows with null absorption coefficient. Based on this representation, the integration of Eq. (1) across the spectral interval corresponding to a single gray gas results in (Modest, 1991)

$$\frac{\mathrm{d}I_j}{\mathrm{d}s} = -\kappa_j I_j + \kappa_j a_j I_b , \quad (3)$$

where $I_j$ represents the partial intensity of gas $j$, while $\kappa_j$ is its absorption coefficient, and $a_j$ its emission weighting coefficient, which represents the fraction of blackbody energy that lies within the spectral intervals corresponding to gas $j$. The total intensity is determined after Eq. (3) has been solved for each gray gases (as well as for the transparent windows, to which the index $j = 0$ is assigned) as a sum of all partial intensities, $I = \sum_{j=0}^{J} I_j$.

The dependence of $\kappa_j$ and $a_j$ on the local thermodynamic state of the medium is typically determined by fitting the total emittance to some reference data. Several WSGG formulations, differing on how this dependence is expressed, have been developed so far, usually applicable to a specific range of applications (e.g., air-fuel combustion at atmospheric conditions, oxy-fuel combustion, sooting flames). Here, some of the most widely used, contemporaneous WSGG correlations are considered: the formulation of Dorigon *et al.*, 2013, applicable to methane-air combustion; the superposition methodology proposed by Cassol *et al.*, 2014; the model by Yin, 2013, that encompasses many different products of air-fuel combustion; and the formulations of Kangwanpongpan *et al.*, 2012, and Bordbar *et al.*, 2014, that were originally developed for oxy-fuel combustion. Each one of these formulations is briefly described below.

- Bordbar *et al.*, 2014 (B. *et al.*): In this formulation, besides depending on the local temperature and partial pressure of the participating medium, the WSGG coefficients also depend on the ratio between the mole fractions of $H_2O$ and $CO_2$, thus making it possible to account for media where this ratio varies (as it is the case in real combustion applications).
- Cassol *et al.*, 2014 (C. *et al.*): The formulation uses a particular formulation where WSGG coefficients for the individual participating species (here, $H_2O$ and $CO_2$) are superposed through statistical arguments. Therefore, it can also account for scenarios where the $H_2O/CO_2$ mole fraction ratio varies.
- Dorigon *et al.*, 2013 (D. *et al.*): It accounts for $H_2O$-$CO_2$ mixture with fixed mole fraction ratio.
- Johansson *et al.*, 2011 (J. *et al.*): It is similar to that of Bordbar *et al.*, 2014. However, while the latter was developed specifically for oxy-fuel scenarios, this one allows for both air-fuel and oxy-fuel conditions.
- Kangwanpongpan *et al.*, 2012 (K. *et al.*): It introduces two formulations. In the first, coefficients are available for fixed values of the $H_2O/CO_2$ mole fraction ratio, similarly to Dorigon *et al.*, 2013. In the second, the coefficients depend on that ratio, in a similar manner as Bordbar *et al.*, 2014.
- Yin, 2013 (Y. *et al.*): It is similar to the WSGG formulation of Dorigon *et al.*, 2013, but its coefficients were generated based on a different (and less up-to-date) spectral database.

### 2.4 Turbulence-radiation interaction (TRI)

The TRI arises from the highly non-linear coupling between fluctuations of the temperature and medium composition and fluctuations of the radiation intensity (Coelho, 2007). To illustrate this, consider the time-averaging of Eq. (1), which leads to

$$\frac{\mathrm{d}\overline{I_\eta}}{\mathrm{d}s} = -\overline{\kappa_\eta I_\eta} + \overline{\kappa_\eta I_{b\eta}}\,, \tag{4}$$

where the time-averaging operation is represented by the overbar. In the presence of turbulent fluctuations, the correlations that appear on the right-hand side of this equation often cannot be neglected—i.e., $\overline{\kappa_\eta I_\eta} \neq \overline{\kappa_\eta}\,\overline{I_\eta}$ and $\overline{\kappa_\eta I_{b\eta}} \neq \overline{\kappa_\eta}\,\overline{I_{b\eta}}$. Moreover, the values of both $\overline{\kappa_\eta}$ and $\overline{I_{b\eta}}$ may differ significantly from these quantities evaluated at the mean temperature and mean medium composition. These two factors combined explain the large errors that occur when the mean radiation field is solved on the basis of mean quantities only, as it is common in RANS simulations of turbulent combustion. Comprehensive reviews on the state-of-the-art of TRI studies and modeling are reported in Coelho (2007), and Modest and Haworth (2016).

To reduce the complexity of the problem while still partially capturing the TRI effects, this paper invokes the OTFA for modeling $\overline{\kappa_\eta I_\eta}$. This approximation simplifies the mean absorption term by neglecting the cross-correlation between the absorption coefficient and the local intensity, yielding $\overline{\kappa_\eta I_\eta} = \overline{\kappa_\eta}\,\overline{I_\eta}$. The validity of such approximation has been verified for a number of non-sooting turbulent flames (Coelho, 2007). The model developed by Snegirev, 2004, is adopted for the emission term, originally introduced for approximating the mean total emission and given as

$$\overline{\kappa_P I_b} = \overline{\kappa_P} I_b(\overline{T}) \left( 1 + 6 C_{TRI,1} \frac{\overline{T'^2}}{\overline{T}^2} + 4 C_{TRI,2} \frac{\overline{T'^2}}{\overline{\kappa_P}\,\overline{T}} \left. \frac{\partial \kappa_P}{\partial T} \right|_{\overline{T}} \right), \tag{5}$$

where the total blackbody intensity evaluated at the local mean temperature is represented by $I_b(\overline{T})$, and $C_{TRI,1}$ (= 2.5) and $C_{TRI,2}$ are the constants of the model. As it was done in previous applications of Snegirev's model—as, for example, in the series of studies by Krishnamoorthy and collaborators (Krishnamoorthy, 2012, 2010; Krishnamoorthy *et al.*, 2005b,a)—the last term of Eq. (5) is neglected by setting $C_{TRI,2} = 0$, in which case the model can be straightforwardly applied for approximating $\overline{\kappa_\eta I_{b\eta}}$,

$$\overline{\kappa_\eta I_{b\eta}} = \overline{\kappa_\eta} I_{b\eta}(\overline{T}) \underbrace{\left( 1 + 6 C_{TRI,1} \frac{\overline{T'^2}}{\overline{T}^2} \right)}_{\beta}, \tag{6}$$

where the Planck function evaluated at the mean temperature is represented by $I_{b\eta}(\overline{T})$. Assuming the term within parenthesis in the above equation as an emission-TRI correction factor $\beta$, the final form of the time-averaged (spectral-based)

RTE solved in this study is given as

$$\frac{d\overline{I_\eta}}{ds} = -\overline{\kappa_\eta}\overline{I_\eta} + \beta\overline{\kappa_\eta} I_{b\eta}(\overline{T}) \,. \tag{7}$$

In an analogous manner, the time-averaged form of the RTE in the framework of the WSGG model is obtained by time-averaging Eq. (3):

$$\frac{d\overline{I_j}}{ds} = -\overline{\kappa_j I_j} + \overline{\kappa_j a_j I_b} \,. \tag{8}$$

Following similar modeling approaches as those adopted for Eq. (4), the above equation becomes

$$\frac{d\overline{I_j}}{ds} = -\overline{\kappa_j}\overline{I_j} + \beta\overline{\kappa_j} a_j(\overline{T}) I_b(\overline{T}) \,, \tag{9}$$

with $a_j(\overline{T})$ the weighting coefficient evaluated at the mean temperature. For $\overline{\kappa_j}$, as well as for $\overline{\kappa_\eta}$ in Eq. (7), the value of the quantity evaluated at the mean temperature and mean medium composition is used for the present calculations.

## 3. METHODOLOGY

For the purpose of testing the accuracy of the spectral models in the absence and presence of TRI, the RTE was solved using the discrete ordinate method (DOM), different from the domain used in a previous study (Gomes *et al.*, 2020) that used the line-of-sight domain, now is used a one-dimensional (1D) domain. Seven WSGG models are simulated together with the LBL model. These models are simulated for three different levels of TRI, characterized by intensities of temperature fluctuations (or turbulent intensities, T.I.) of 0 %, representing the absence of TRI, 40 % and 60 % representing the presence of the TRI in the flow. In order to combine the turbulence and radiation, the temperature variance is calculated Eq. (10), then through the artificial introduction of a temperature field and the turbulent intensity (T.I.) in the $\beta$ Eq. (11) term.

$$T'^2 = ((T.I.)T)^2 \,, \tag{10}$$

$$\beta = 1 + 6C_{TRI,1}\frac{\overline{T'^2}}{\overline{T}^2} \,, \tag{11}$$

The temperature profiles, used according to Dorigon *et al.* (2013), are shown below

$$T(x^*) = 400\,\mathrm{K} + (1400\,\mathrm{K})\sin^2(\pi x^*) \,, \tag{12}$$

$$T(x^*) = 400\,\mathrm{K} + (1400\,\mathrm{K})\sin^2(2\pi x^*) \,, \tag{13}$$

$$T(x^*) = \begin{cases} 880\,\mathrm{K} + (920\,\mathrm{K})\sin^2(2\pi x^*) & if \;\; x^* \leq 0.25 \\ 400\,\mathrm{K} + (1400\,\mathrm{K})\left\{1 - \sin^{3/2}\left[\frac{2}{3}\pi(x^* - 0.25)\right]\right\} & if \;\; x^* > 0.25 \end{cases} \tag{14}$$

The term $x^*$ represents a middle point of the path, and can be defined by $x^* = x/l$, where $x$ is the point in the beginning of path and $l$ is the final point (considering $l = 1$ m). The profiles of molar concentrations of $CO_2$ for the six cases are shown below

$$Y_{CO_2}(x^*) = 0.1 \,, \tag{15}$$

$$Y_{CO_2}(x^*) = 0.2\sin^2(\pi x^*) \,, \tag{16}$$

$$Y_{CO_2}(x^*) = 0.2\sin^2(2\pi x^*) \,, \tag{17}$$

$$Y_{CO_2}(x^*) = \begin{cases} 0.25\sin^2(2\pi x^*) & if \;\; x^* \leq 0.25 \\ 0.25\left\{1 - \sin\left[\frac{3}{2}\pi(x^* - 0.25)\right]\right\} & if \;\; x^* > 0.25 \end{cases} \tag{18}$$

Altogether there are three profiles of temperature profiles and of molar fractions concentrations, combined in six cases, according to the combinations indicated in Table 1.

It is worth noting that the increase in turbulence intensity from 0 % to up to 60 % was made in order to find out if there will be variations in the errors in computing the heat source and radiative heat flux with the different WSGG models.

Table 1. Cases used by Dorigon *et al.*, 2013

| Case | 1 | 2 | 3 | 4 | 5 | 6 |
|---|---|---|---|---|---|---|
| Temperature profile | Eq. (12) | Eq. (13) | Eq. (14) | Eq. (12) | Eq. (13) | Eq. (14) |
| Molar concentration profile | Eq. (15) | Eq. (15) | Eq. (15) | Eq. (16) | Eq. (17) | Eq. (18) |

Table 2. Differences between LBL and WSGG models for different levels of temperature fluctuation intensity, values without parentheses represent the maximum difference of errors, values with parentheses represent the average difference between errors

| | B. *et al.* | C. *et al.* | D. *et al.* | J. *et al.* | K. *et al.*(Fix.) | K. *et al.*(Var.) | Y. *et al.* |
|---|---|---|---|---|---|---|---|
| Source: | | | | | | | |
| T.I. = 0 % | 6.19 | 9.09 | 6.03 | 5.32 | 7.21 | 11.73 | 8.67 |
| | (4.25) | (5.76) | (3.86) | (2.22) | (5.32) | (7.75) | (5.02) |
| T.I. = 40 % | 8.35 | 8.92 | 7.98 | 7.62 | 8.35 | 11.56 | 8.49 |
| | (4.22) | (5.73) | (3.85) | (2.25) | (5.28) | (7.70) | (5.02) |
| T.I. = 60 % | 8.76 | 8.96 | 8.36 | 8.07 | 8.77 | 11.53 | 8.45 |
| | (4.21) | (5.72) | (3.84) | (2.26) | (5.27) | (7.69) | (5.02) |
| Flux: | | | | | | | |
| T.I. = 0 % | 7.52 | 14.87 | 5.83 | 6.59 | 11.62 | 18.45 | 7.32 |
| | (4.09) | (10.34) | (3.19) | (1.41) | (7.27) | (12.42) | (3.82) |
| T.I. = 40 % | 7.24 | 14.50 | 5.56 | 6.79 | 11.30 | 18.11 | 7.10 |
| | (3.89) | (10.06) | (3.04) | (1.50) | (7.02) | (12.16) | (3.75) |
| T.I. = 60 % | 7.18 | 14.43 | 5.51 | 6.83 | 11.24 | 18.04 | 7.05 |
| | (3.85) | (10.00) | (3.02) | (1.52) | (6.97) | (12.11) | (3.74) |

## 4. RESULTS AND DISCUSSIONS

Figures 1 and 2 present the radiative heat source ($S_r$) and radiative heat flux ($q''_R$) obtained with the LBL integration and the six WSGG models mentioned in the previous section.

Note that the two formulations of the model of Kangwanpongpan *et al.*, 2012 are included: the one for a fixed mole fraction ratio and the one for a variable mole ratio. The results shown in Figs. 1 and 2 correspond to Case 1; the other cases yielded similar results and will only be briefly discussed here, for the sake of conciseness.

From Figs. 1 and 2, it is possible to see the increase in the radiation heat transfer as the turbulence intensity increases. The values of the radiative heat source and flux increase significantly in the presence of the TRI. For instance, in all WSGG models the radiative heat flux in some points presented a difference of approximately $200 \text{kW/m}^2$ when comparing the results with T.I. of 0 % (no-TRI) to those with a T.I. of 40 %, while for T.I. of 60 % the difference reached approximately $400 \text{kW/m}^2$. Regarding the radiative heat source, between T.I. of 0 % and 40 %, the WSGG models showed a maximum difference of approximately $1500 \text{kW/m}^3$, while the maximum difference between 0 % and 60 % is approximately $3000 \text{kW/m}^3$.

The Johansson *et al.*, 2011, WSGG model presents values closer to the LBL model values than the other WSGG models. The maximum and domain-averaged values of the normalized errors of the seven WSGG models are reported in Table 2 for more details. Evaluating the results of all simulated WSGG models, the following information was obtained: when related to the source term, the WSGG model of Johansson *et al.*, 2011, was closer to the LBL method, with an average mean error of 2.2 %, followed by Dorigon *et al.*, 2013; Bordbar *et al.*, 2014; Yin, 2013; Kangwanpongpan *et al.*, 2012 (Fixed), Cassol *et al.*, 2014; Kangwanpongpan *et al.*, 2012 (Variable), with the respective approximate values of 3.8 %, 4.2 %, 5 %, 5.3 %, 5.7 % and 7.7 %. Regarding the radiative heat flux, the mean of the average errors presented an order similar to the models in the source term, changing the order only between the Yin, 2013 and Bordbar *et al.*, 2014 models, the following order being J. *et al.*, D. *et al.*, Y. *et al.*, B. *et al.*, K. *et al.*(Fixed), C. *et al.* and K. *et al.*(Variable), with the respective values 1.5 %, 3.1 %, 3.7 %, 4 %, 7.1 %, 10 % and 12.12 %.

It is also worth noting that the models with less accuracy are the ones developed for a varying $H_2O/CO_2$ mole fraction ratio, Kangwanpongpan *et al.*, 2012(Variable) and Cassol *et al.*, 2014 , which uses the superposition methodology. This

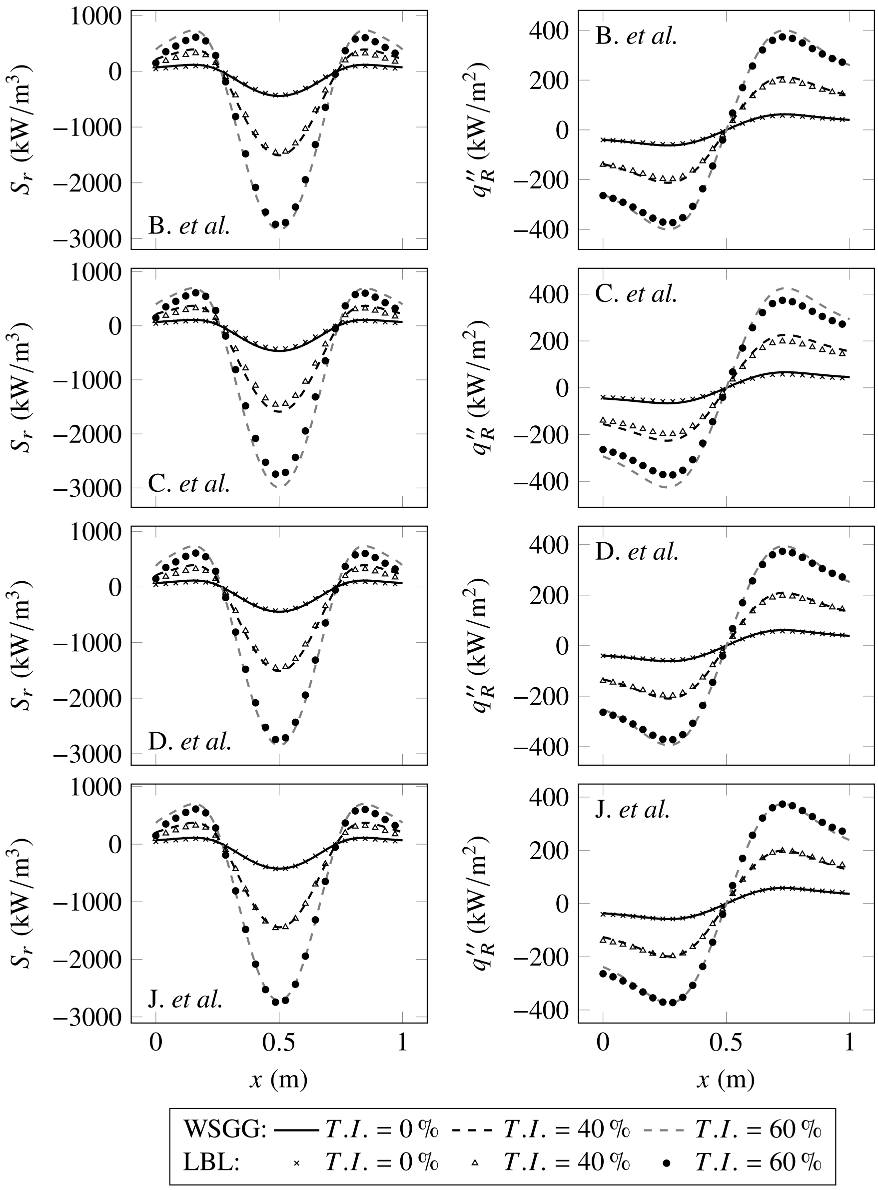


Figure 1. Case 1 - Different source term and radiative heat flux for models WSGG (1)

is to be expected, since in the cases considered here the mole fraction ratio is always constant. On the other hand, it is important to highlight that the Bordbar *et al.*, 2014 model also uses coefficients for ratios of variable molar fractions, but it presented more accurate values than even the Yin, 2013, model.

In general, there is no specific influence of T.I. on the accuracy of the WSGG model, and, in fact, all of the tested formulations behave similarly when subjected to the effects of TRI. A similar finding was made in a previous study by us (Gomes *et al.*, 2020), which studied the accuracy of different WSGG models, when subjected to varying levels of turbulence in estimating the radiation intensity along several line-of-sights for the Sandia flame D.

To illustrate how the findings for Case 1 are similar to those for the other cases, Fig. 3 compares the results for the radiative heat source and the radiative heat flux obtained by the WSGG model of Dorigon *et al.*, 2013, to those of the LBL solution for all other test cases. From these results it was possible to see that this model has a good accuracy for all cases and all turbulence levels. Interestingly, this contradicts the finding of Gomes *et al.*, 2020, where the model of Dorigon *et al.*, 2013 performed poorly for predicting the radiation intensity along line-of-sights.

## 5. CONCLUSIONS

Based on the obtained results, it can be concluded that there is no influence of the intensity of the turbulence on the accuracy of the WSGG models, although there is a subtle improvement in accuracy when the effects of TRI are

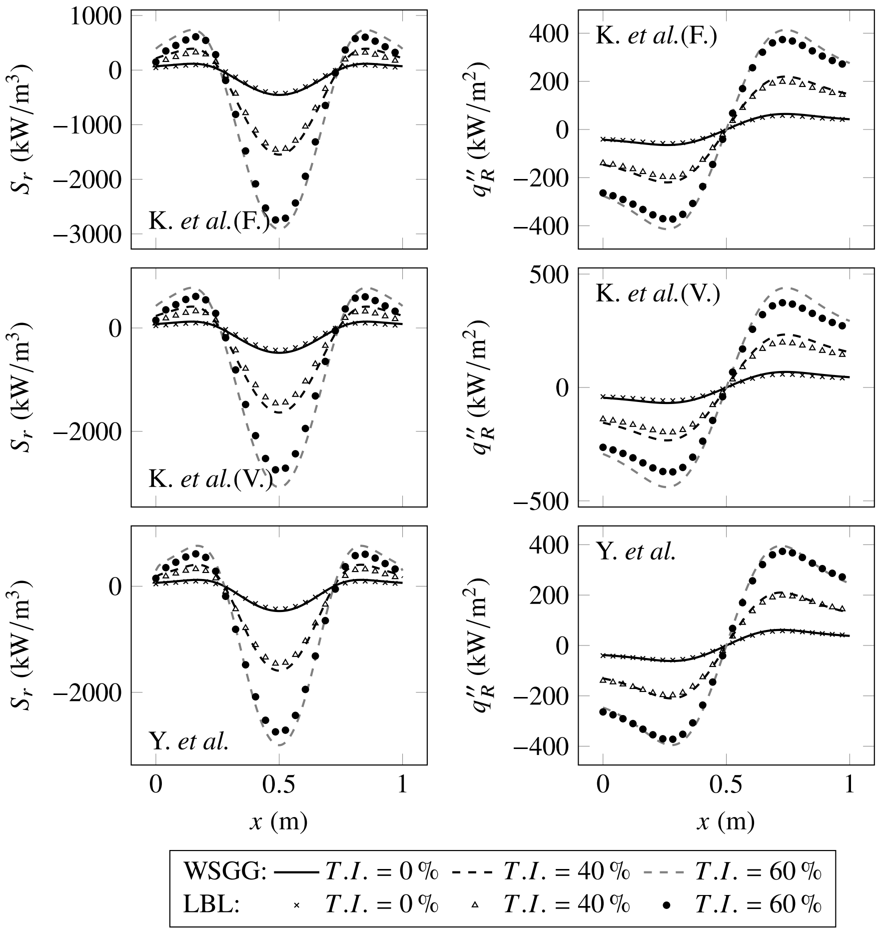


Figure 2. Case 1 - Different source term and radiative heat flux for models WSGG (2)

increased. The tested WSGG models presented average error percentage values when compared to the LBL method around approximately 5 % for both the source term and the radiative heat flux, with the models with variable coefficients being the most distant. It should be highlighted that the Johansson *et al.*, 2011 model presented the most accurate results, while the Bordbar *et al.*, 2014 model presented the best results among the models that use variable coefficients.

## 6. ACKNOWLEDGMENTS

Author BLZG thanks CAPES for a masters scholarship. Author GCF thanks CNPq for a doctoral scholarship. Author FHRF thanks CNPq for research grant 302686/2017-7.

## 7. REFERENCES

Bordbar, M.H., Wecel, G. and Hyppänen, T., 2014. "A line by line based weighted sum of gray gases model for inhomogeneous CO2-H2O mixture in oxy-fired combustion". *Combustion and Flame*, Vol. 161, No. 9, pp. 2435–2445. doi:10.1016/j.combustflame.2014.03.013.

Cassol, F., Brittes, R., França, F.H. and Ezekoye, O.A., 2014. "Application of the weighted-sum-of-gray-gases model for media composed of arbitrary concentrations of $H_2O$, $CO_2$ and soot". *International Journal of Heat and Mass Transfer*, Vol. 79, pp. 796–806. doi:10.1016/j.ijheatmasstransfer.2014.08.032.

Coelho, P.J., 2007. "Numerical simulation of the interaction between turbulence and radiation in reactive flows". *Progress in Energy and Combustion Science*, Vol. 33, No. 4, pp. 311–383. doi:10.1016/j.pecs.2006.11.002.

Dorigon, L.J., Duciak, G., Brittes, R., Cassol, F., Galarça, M. and França, F.H., 2013. "WSGG correlations based on HITEMP2010 for computation of thermal radiation in non-isothermal, non-homogeneous $H_2O/CO_2$ mixtures". *International Journal of Heat and Mass Transfer*, Vol. 64, pp. 863–873. doi:10.1016/j.ijheatmasstransfer.2013.05.010.

Gomes, B.d.L.Z., Fraga, G.C. and França, F.H.R., 2020. "Evaluation of the accuracy of thermal radiation models in the absence and presence of turbulent fluctuations".

Hall, R.J. and Vranos, A., 1994. "Efficient calculations of gas radiation from turbulent flames". *International Journal of*

*Heat and Mass Transfer*, Vol. 37, No. 17, pp. 2745–2750. doi:10.1016/0017-9310(94)90391-3.

Howell, J.R., Mengüç, M.P. and Siegel, R., 2016. *Thermal Radiation Heat Transfer*. CRC press, 6th edition.

Johansson, R., Leckner, B., Andersson, K. and Johnsson, F., 2011. "Account for variations in the H2O to CO2 molar ratio when modelling gaseous radiative heat transfer with the weighted-sum-of-grey-gases model". *Combustion and Flame*, Vol. 158, No. 5, pp. 893–901. doi:10.1016/j.combustflame.2011.02.001.

Kabashnikov, V. and Kmit, G., 1979. "Influence of turbulent fluctuations on thermal radiation". *Journal of Applied Spectroscopy*, Vol. 31, No. 2, pp. 963–967. doi:10.1007/bf00614832.

Kangwanpongpan, T., França, F.H., da Silva, R.C., Schneider, P.S. and Krautz, H.J., 2012. "New correlations for the weighted-sum-of-gray-gases model in oxy-fuel conditions based on HITEMP 2010 database". *International Journal of Heat and Mass Transfer*, Vol. 55, No. 25, pp. 7419–7433. doi:10.1016/j.ijheatmasstransfer.2012.07.032.

Krishnamoorthy, G., 2010. "A new weighted-sum-of-gray-gases model for $CO_2$-$H_2O$ gas mixtures". *International Communications in Heat and Mass Transfer*, Vol. 37, No. 9, pp. 1182–1186. doi:doi.org/10.1016/j.icheatmasstransfer.2010.07.007.

Krishnamoorthy, G., 2012. "A comparison of angular discretization strategies for modeling radiative transfer in pool fire simulations". *Heat Transfer Engineering*, Vol. 33, No. 12, pp. 1040–1051. doi:10.1080/01457632.2012.659626.

Krishnamoorthy, G., Borodai, S., Rawat, R., Spinti, J. and Smith, P.J., 2005a. "Numerical modeling of radiative heat transfer in pool fire simulations". In *Heat Transfer, Part A*. ASME, Vol. 2005, pp. 327–337. ISBN 0-7918-4221-5. doi:10.1115/IMECE2005-81095.

Krishnamoorthy, G., Rawat, R. and Smith, P.J., 2005b. "Parallel computations of nongray radiative heat transfer". *Numerical Heat Transfer: Part B: Fundamentals*, Vol. 48, No. 2, pp. 191–211. doi:10.1080/10407790590963631.

Modest, M.F., 1991. "The weighted-sum-of-gray-gases model for arbitrary solution methods in radiative transfer". *Journal of Heat Transfer*, Vol. 113, No. 3, pp. 650–656. doi:10.1115/1.2910614.

Modest, M.F., 2013. *Radiative Heat Transfer*. Academic Press.

Modest, M.F. and Haworth, D.C., 2016. *Radiative Heat Transfer in Turbulent Combustion Systems: Theory and Applications*. Springer.

Rothman, L., Gordon, I., Barber, R., Dothe, H., Gamache, R., Goldman, A., Perevalov, V., Tashkun, S. and Tennyson, J., 2010. "Hitemp, the high-temperature molecular spectroscopic database". *Journal of Quantitative Spectroscopy and Radiative Transfer*, Vol. 111, No. 15, pp. 2139–2150. doi:10.1016/j.jqsrt.2010.05.001.

Snegirev, A.Y., 2004. "Statistical modeling of thermal radiation transfer in buoyant turbulent diffusion flames". *Combustion and Flame*, Vol. 136, No. 1, pp. 51–71. doi:10.1016/j.combustflame.2003.09.005.

Yin, C., 2013. "Refined weighted sum of gray gases model for air-fuel combustion and its impacts". *Energy and Fuels*, Vol. 27, No. 10, pp. 6287–6294. doi:10.1021/ef401503r.

## 8. RESPONSIBILITY NOTICE

The authors are solely responsible for the printed material included in this paper.

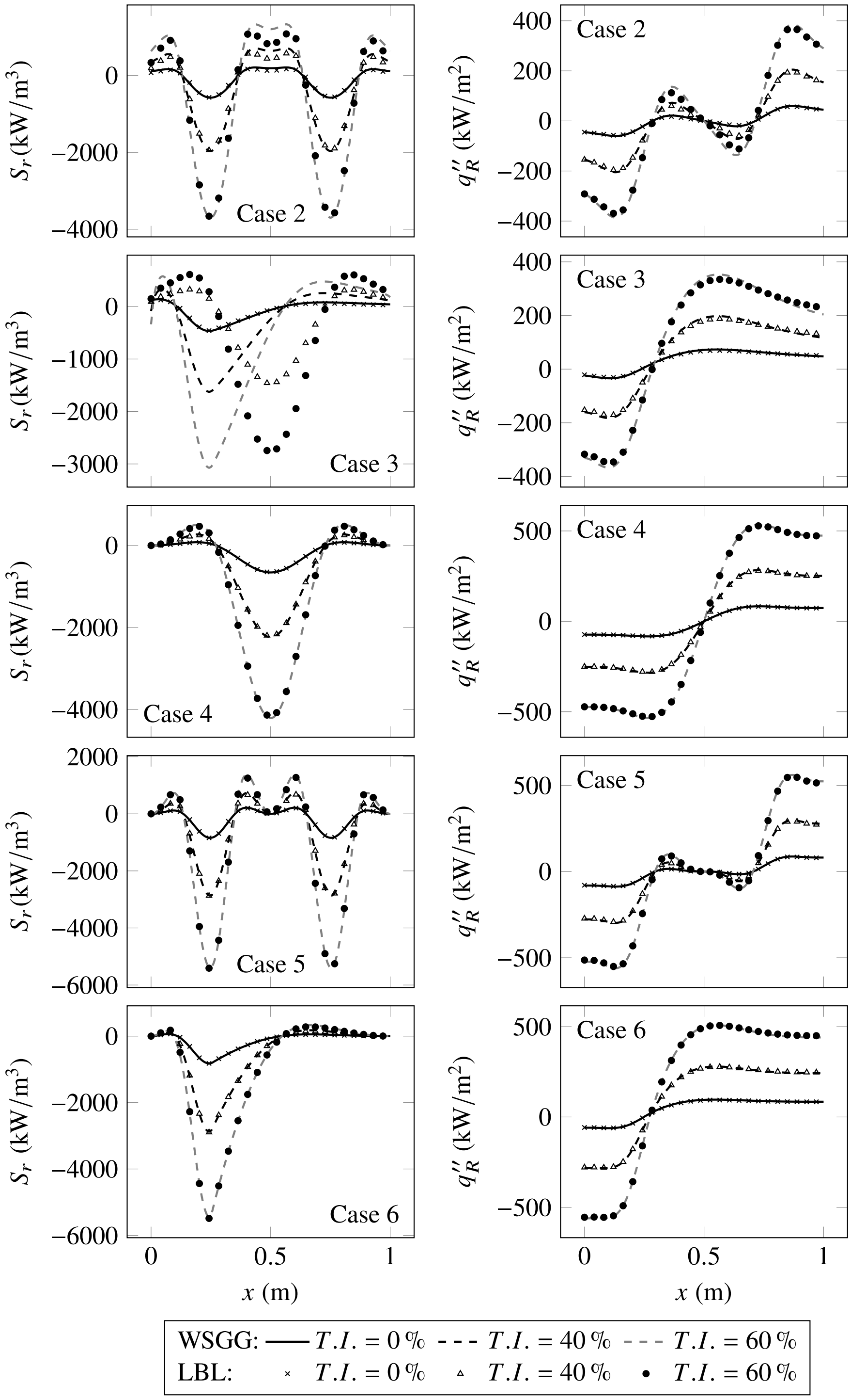


Figure 3. Cases 2-6 - Different source term and radiative heat flux for Dorigon *et al.*, 2013